

ments show that the conduction band consists of six ellipsoidal minima centered on the reflection planes of the crystal. Two of the major axes of the ellipsoids lie in the reflection planes and make angles of 25° with respect to the trigonal and bisectrix directions, respectively. In addition, there is a second conduction band consisting of one or more minima lying approximately 30 meV above the first set. The shape of the constant-energy surfaces for the lower band is independent of the carrier concentration for total carrier concentrations between 9×10^{17} and 2.4×10^{19} . The average effective

mass is reasonably close to that obtained from Faraday-rotation experiments.

ACKNOWLEDGMENTS

Thanks are due to Dr. G. B. Brandt for his help in making the initial measurements and to D. Zupon for his assistance in preparing the samples used in these experiments. Two of us (R.B.M. and J.A.R.) gratefully acknowledge the support of the National Science Foundation.

Intensity of Forbidden Neutron Reflections Simulated by Multiple Bragg Reflection*

D. A. KOTTWITZ

Battelle Memorial Institute, Pacific Northwest Laboratory, Richland, Washington 99352

(Received 29 May 1968)

Exploratory measurements have been made of the intensity of several forbidden neutron reflections simulated by multiple Bragg reflection in large single crystals. The (0003) and (0001) reflections were studied in a beryllium crystal with mosaic $<0.25^\circ$ and the (200) in a germanium crystal with mosaic $<0.02^\circ$. Double-crystal methods were used with a triple-axis spectrometer. Large amounts of order contamination were treated by means of resonance absorption filters and least-squares analysis of overdetermined equations. To minimize the effect of peculiarities of individual specimens, the results are presented as intensity ratios. Simulated reflections were observed to have $1/60$ to $1/3$ the intensity of ordinary Bragg reflections. No conclusive evidence was found for an intrinsic component due to the forbidden reflections themselves; the Be simulations were at least 200 to 700 times, and the Ge simulations at least 15 to 60 times, more intense than the corresponding intrinsic components. Caution must be used in applying these results to other specimens.

I. INTRODUCTION

FOR several decades the phenomenon of multiple Bragg reflection (MBR) (often referred to as multiple diffraction or simultaneous reflection) has been studied experimentally and theoretically for x rays, electrons, and neutrons; an extensive literature has been reviewed recently.¹ Although a number of beneficial uses have been suggested and demonstrated, it is probably fair to say that the effect has been mostly a nuisance. This is true for both spectrometry and structure studies, in which perturbed intensities of ordinary reflections and confusing appearances of forbidden reflections may occur. In fact much recent work has dealt with the question of avoiding or minimizing the effects of MBR.

However, the possibility of producing extremely monochromatic, semiparallel beams of x rays and slow neutrons at fixed wavelengths by means of MBR in certain types of perfect single crystals has been pointed

out recently.² The proposed method is based on effects which occur at particular crystal orientations in cases of pure "Umweganregung"³; that is, when a strongly forbidden Bragg reflection is simulated by MBR. Such high-quality beams, particularly of slow neutrons, have several potential uses in research, provided they are intense enough. Although several investigations concerned with the intensity of simulated neutron reflections have been reported,⁴⁻⁶ it is difficult to relate their results to the reflectivity of large crystals, which is the basic quantity of interest in monochromatization.

The purpose of this paper is to present the results of a preliminary experimental survey of several simulated neutron reflections, the main goals of which were (1) to determine the general order of magnitude of their intensity and (2) to identify some of the more intense peaks for subsequent detailed study. The measurements

² D. A. Kottwitz, *Acta Cryst.* **A24**, 117 (1968).

³ M. Renninger, *Z. Physik* **106**, 141 (1937).

⁴ H. J. Hay, Atomic Energy Research Establishment Report No. AERE-R 2982, 1959 (unpublished).

⁵ R. M. Moon and C. G. Shull, *Acta Cryst.* **17**, 805 (1964).

⁶ R. R. Spencer, Atomic Energy Commission Research and Development Report No. IDO-17029, 1964 (unpublished).

* Work performed under U. S. Atomic Energy Commission Contract No. AT(45-1)-1830.

¹ Yu. S. Terminasov and L. V. Tuzov, *Usp. Fiz. Nauk* **83**, 223 (1964) [English transl.: *Soviet Phys.—Usp.* **7**, 434 (1964)].

were made on single crystals of beryllium and germanium; each of these elements represents an important type of crystal structure in which the simulation of forbidden reflections by MBR is a prominent characteristic.

The properties of simulated reflections are summarized in Sec. II, the experimental methods are described in Sec. III, and details of the measurements on Be and Ge are presented in Secs. IV and V. A discussion of the results is given in Sec. VI.

II. PROPERTIES OF SIMULATED REFLECTIONS

The physics and geometry involved in the simulation of a forbidden reflection by MBR in a single crystal are shown schematically in Fig. 1. For a given value of the azimuthal angle α and a given pair of secondary and tertiary reflections, there is a value of the Bragg angle θ (relative to the forbidden primary planes) at which the secondary and tertiary planes cooperate to produce a doubly reflected beam that appears to have been reflected from the primary planes. For pictorial clarity the sketch in Fig. 1 is oversimplified in two respects. First, the double reflection process occurs in parallel (dynamically) and not only in series. Secondly, for forbidden reflections having high symmetry, e.g., Ge(200), it often happens that the conditions for simulation are *identical* for distinct secondary-tertiary pairs; in such cases there are two or more intermediate beams.

The measurement of the reflectivity of such simulated reflections is not a simple, straightforward matter. It is well known that the reflectivity of crystals for neutrons is a structure-sensitive property.⁷ However, the effects of peculiarities of a particular specimen may be minimized by measuring the intensity of simulated reflections relative to the intensity of similarly oriented ordinary Bragg reflections in the same crystal.

Unfortunately this step introduces a fundamental difficulty due to differences between the geometrical conditions for ordinary reflections and simulated reflections. The situation for ordinary reflections is shown in the upper part of Fig. 2, where the point O is the origin of the reciprocal lattice, \mathbf{K}_1 is the reciprocal-lattice vector corresponding to the primary (ordinary) reflection, while \mathbf{k}_0 and \mathbf{k}_1 are the incident and reflected wave vectors, respectively. The Laue-Bragg condition for reflection is satisfied whenever the foot C of the incident wave vector lies on the plane perpendicular to \mathbf{K}_1 . Actually, the reflectivity of a macroscopic crystal is finite for wave vectors beginning in the immediate neighborhood of the plane, the effective "thickness" of the region being proportional to the structure factor for perfect crystals and to the mosaic spread for imperfect crystals. To select a pencil of directions for a beam, collimation must be provided in

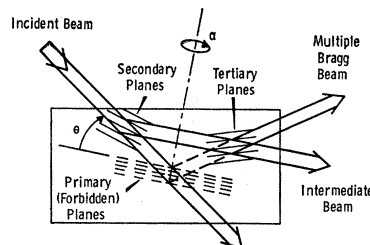


FIG. 1. Schematic picture of simulation of a forbidden reflection by MBR in a single crystal. Although this oversimplified sketch suggests that the multiple processes occur successively, they actually occur simultaneously.

two directions; this is represented by a small rectangle surrounding point C .

In contrast the more complicated geometry of simulated reflections is shown in the lower part of Fig. 2. In addition to the previous elements we find the secondary and tertiary reciprocal-lattice vectors \mathbf{K}_2 and \mathbf{K}_3 , the corresponding perpendicular-bisector planes, and the intermediate wave vector \mathbf{k}_2 . The conditions for MBR are satisfied whenever the foot C of the incident wave vector lies on the line AB , which is the common intersection of all three perpendicular bisectors. Thus, we see that the simulation of forbidden reflections by MBR is not complete; it occurs only when the foot of the incident wave vector lies on certain lines in the primary plane. As before, the region of finite reflectivity is broadened for both perfect and imperfect crystals, but now it is threadlike instead of sheetlike. To define a pencil of beam directions it is sufficient to provide collimation in one direction, as indicated in the figure.

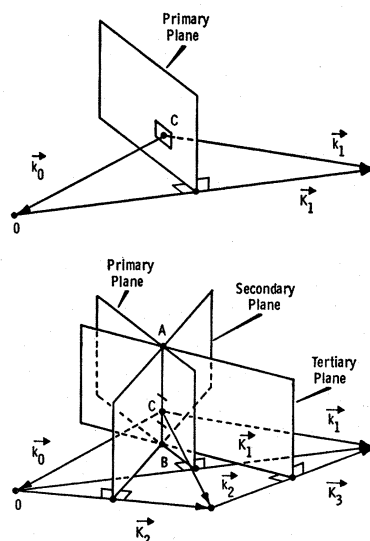


FIG. 2. Detailed diffraction geometry including the incident, primary, and secondary neutron wave vectors \mathbf{k}_0 , \mathbf{k}_1 , and \mathbf{k}_2 ; and the reciprocal-lattice vectors \mathbf{K}_1 , \mathbf{K}_2 , and \mathbf{K}_3 , corresponding to the primary, secondary, and tertiary reflections. The upper portion shows ordinary Bragg reflection for an allowed primary reflection. The lower portion shows how the cooperative action of the secondary and tertiary reflections simulates a forbidden primary reflection along the line AB .

⁷ G. E. Bacon, *Neutron Diffraction* (Clarendon Press, Oxford, England, 1962), 2nd ed., Chap. III, p. 55.

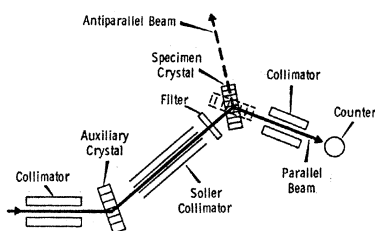


FIG. 3. Schematic plan view of experimental arrangement.

The difference in dimensionality of the regions of finite reflectivity for ordinary and simulated reflections complicates the comparison of reflectivities. For example, assuming that the crystal mosaic spread is much smaller than the collimation angles, the intensity of an ordinary reflection is proportional to a solid angle (or area) while that of a simulated reflection is proportional to a planar angle (or length). Partly for this reason and partly for others to be discussed later, the present measurements were done with the aid of an auxiliary crystal. By this means the reflecting regions in reciprocal space can be made to have roughly the same threadlike volume, making it possible to get rough estimates of ratios of detailed (not integrated) reflectivities.

A separate but related problem arises when a nominally "forbidden" reflection has a nonzero structure factor. This may happen in cases of deviation from an assumed crystal symmetry. It is then important to measure the ratio of the simulated reflectivity to the hopefully weak intrinsic reflectivity of the forbidden reflection, since the latter contributes an inseparable contamination in high-resolution monochromatization.²

Since a forbidden reflection may be simulated by many different secondary-tertiary pairs having various orientations, the primary plane in Fig. 2 should be criss-crossed by many threads at which simulation occurs. Thus some degree of coarse collimation is needed to isolate a particular simulation for use or study.

III. EXPERIMENTAL METHODS

The methods of double-crystal spectrometry⁸ were used to study the simulated reflections. There are two advantages to using an auxiliary crystal in addition to that mentioned previously. First, an auxiliary crystal with a small mosaic spread provides better angular resolution than ordinary collimating tubes. Thus the intrinsic reflectivity of the forbidden reflection may be studied in wider valleys between the simulation peaks. Secondly, an auxiliary crystal can often be chosen to discriminate against relatively intense higher (and sometimes lower) orders of ordinary Bragg reflection which inevitably accompany simulated reflections. For

example, if the Ge(111) reflection is used to study simulations of Be(0001), then the small reflectivity of Ge(222) reduces the otherwise intense second-order contamination due to Be(0002).

The measurements were performed with the Hanford triple-axis neutron spectrometer; a schematic plan view of the setup is shown in Fig. 3. The crystals were mounted at the first and third axes, the second arm being held at its straight-through position. For the Be measurements the specimen was at the first axis, while for the Ge measurements it was at the third axis. Thus, the auxiliary crystal functioned either as an analyzer or a monochromator. The most significant collimation was produced by a set of Soller slits located between the crystals and having a horizontal width $\approx 0.09^\circ$ and vertical width $\approx 0.8^\circ$ (all widths given are full width at half-maximum). The beam was 2.5 cm high and 1.9 cm wide. The counting system consisted of a BF_3 detector and conventional electronics.

A germanium crystal, 0.62 cm thick, was used as an auxiliary crystal in all measurements except a preliminary one in which copper was used. The Ge(111) reflection was employed in an asymmetrical transmission orientation. A separate set of measurements by means of two other germanium crystals of similar quality showed that the angular width $\Delta\theta$ of the reflectivity curve for Ge(111) was $\approx 0.02^\circ$.

In the course of measurements of the simulated reflections a variety of crystal and arm rocking curves were taken in both parallel and antiparallel positions (see Fig. 3). However, most of the results, including those presented below, were obtained by a special double-crystal rocking technique in which both crystals (and arms) are rotated simultaneously to scan a particular wavelength interval. At each angular setting of the specimen crystal a monochromatic probe beam of neutrons having the proper wavelength is thus furnished or transmitted by the auxiliary crystal.

The problem of beam contamination by ordinary Bragg reflections which constitute the various orders of a simulated reflection can be serious even when an auxiliary crystal is used. The most efficient and flexible ways of handling these undesired orders would probably be either (1) removal by a coarse velocity selector⁴ or (2) separation by time-of-flight techniques.⁶ Since these methods were not conveniently available, resonance absorption filters composed of gadolinium, cadmium, erbium, and iridium were used instead. Filters are particularly necessary when it is desired to measure (or set an upper limit for) the intrinsic forbidden intensity in the valleys between simulation peaks. In fact the availability of resonance filters was an important factor in the choice of wavelength intervals to study in the present work.

Sometimes as many as four orders of reflection had to be considered. In such cases it was seldom possible to find four combinations of filters which by themselves enabled a clean, unambiguous analysis of the various

⁸ A. H. Compton and S. K. Allison, *X Rays in Theory and Experiment* (D. Van Nostrand, Inc., New York, 1935), 2nd ed., Chap. IX, p. 709.

orders. To increase the reliability of the filter analysis, an "excessive" number of different filter combinations were used. The resulting set of overdetermined linear equations were then solved by means of a computer program based on least-squares methods.⁹

IV. MEASUREMENTS OF BERYLLIUM REFLECTIONS

The elemental hexagonal close-packed structure has been suggested for high-resolution monochromatization.² Beryllium is an important representative of this structure because its relatively small interatomic spacing provides a supply of small wavelengths. Further interest attaches to beryllium, since unexpected neutron intensities in three different crystals have been attributed to the forbidden (0001); that is, to the intrinsic reflection and not a simulation.¹⁰ An appreciable intrinsic intensity would make such a "forbidden" reflection useless for high-resolution monochromatization. Thus we were led to perform measurements on the forbidden Be(0003) and (0001) reflections.

The specimen Be crystal had a rather irregular shape with average dimensions $\approx 4 \text{ cm} \times 5 \text{ cm} \times 1 \text{ cm}$ (height, width, thickness). Previous measurements had shown its ordinary (0002) reflection to have an angular width $\Delta\theta = 0.26^\circ$. The (0001) planes were roughly parallel to the broad crystal face; thus, the beam geometry was approximately that of symmetrical reflection (Bragg case). It should be emphasized that the Be simulations have not been studied at orientations suitable for high-resolution monochromatization. Since our main interest lay in questions of intensity rather than resolution,

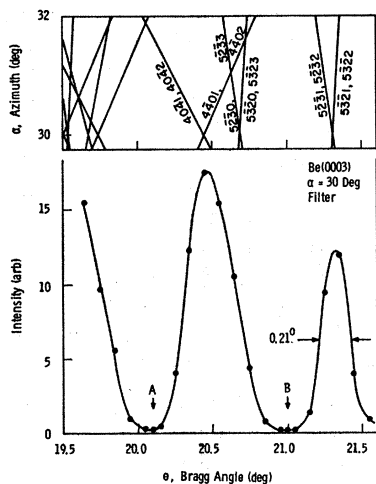


FIG. 4. Simulated Be(0003) reflections near $\theta = 20.5^\circ$. The upper part shows the loci for MBR, with curves labeled by indices of secondary reflections. The lower part shows a special double-crystal rocking curve taken with an erbium filter.

⁹ B. H. Duane, Atomic Energy Commission Research and Development Report No. BNWL-390, 1967 (unpublished).

¹⁰ H. J. Hay, N. J. Pattenden, and P. A. Egelstaff, Acta Cryst. 11, 228 (1958).

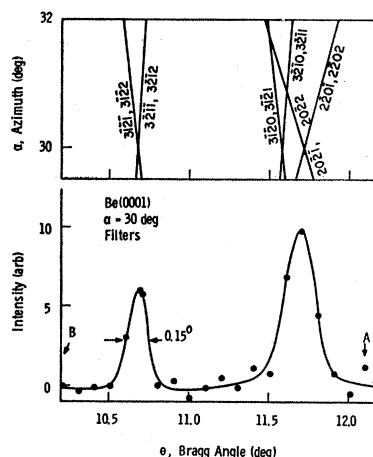


FIG. 5. Simulated Be(0001) reflections near $\theta = 11.0^\circ$. The intensity curve plotted in the lower part is the result of subtracting double-crystal data taken with a gadolinium filter from those taken with a thin cadmium filter.

we did not consider it worthwhile to go through the tedious process of remounting and realignment that would have been necessary. The resulting error in the intensity is small, since the mosaic spread of the specimen is much larger than that of the auxiliary crystal. In all experiments on Be, the (0002) and $(2\bar{1}\bar{1}0)$ planes and their zone axis $[120]$ were vertical, while the plane of scattering was horizontal; this orientation corresponds to $\alpha = 30^\circ$ in Figs. 4 and 5.

The first measurements were done on simulations of Be(0003) in the neighborhood of $\theta = 20.5^\circ$ (see Fig. 4). The upper part of the figure shows the calculated loci of orientations at which simulation of the forbidden reflection occurs. Some of the prominent curves are identified with the indices of the relevant secondary reflections. Note that the curves are double and that they intersect in pairs at $\alpha = 30^\circ$; thus, four secondary reflections act simultaneously there. The lower part of Fig. 4 shows the intensity observed in a special double-crystal traverse at $\alpha = 30^\circ$, using an Er filter and the Ge(111) reflection of the auxiliary crystal in the parallel position. As expected the observed widths of the simulation peaks are due primarily to the rather large mosaic spread of the Be crystal. Additional detailed measurements using Er and Gd filters were made at the peaks and at nearby points A and B in the valleys. As explained in Sec. II similar filter measurements were then made at the same wavelengths for a double-crystal setup in which the "ordinary" Be(0002) reflection replaces the forbidden Be(0003). After the order contamination is removed by the analysis of the filter measurements, we have the following three types of quantities: I_{sim} , the intensity of a simulation peak; I_{int} , the intrinsic intensity of the forbidden reflection; and I_{ord} , the intensity of an ordinary Bragg reflection under similar conditions. The final results are presented in the form of ratios in lines 2 and 3 of Table I, where the unresolved pair of peaks near $\theta = 20.5^\circ$ are lumped

TABLE I. Intensity results for forbidden neutron reflections simulated by multiple Bragg reflection. Bracketed rows correspond to unresolved peaks. The indices of other secondary reflections referred to in column 2 are shown in Figs. 4-6. Column 4 has the intensity ratio for a simulated forbidden reflection relative to an ordinary Bragg reflection. Column 5 has the ratio relative to the intrinsic intensity of the forbidden reflection.

Forbidden reflection	Secondary reflections	Energy (eV)	I_{sim}/I_{ord}	I_{sim}/I_{int}	Aux. crystal reflection
Be(0003)	40 $\bar{4}$ 1+3 others	0.117	1/62	500±100	Cu(200)
	5 $\bar{2}$ 30+3 others	0.115			
	40 $\bar{4}$ 1+3 others	0.117	1/28	380±130	Ge(111)
	5 $\bar{2}$ 30+3 others	0.115			
	5 $\bar{2}$ 31+3 others	0.108	1/50	260±90	Ge(111)
Be(0001)	3 $\bar{1}$ 2 $\bar{1}$ +3 others	0.0464	1/17	>480	Ge(111)
	3 $\bar{1}$ 20+3 others	0.0395	1/11	>730	Ge(111)
	20 $\bar{2}$ 1+3 others	0.0386			
Ge(200)	53 $\bar{3}$, 33 $\bar{3}$	0.0412	1/5	>67	Ge(111)
	35 $\bar{5}$, 15 $\bar{5}$	0.0385	1/18	>16	Ge(111)

together. The results of a preliminary and less complete set of measurements on Be(0003) using a copper auxiliary crystal are given in line 1 of Table I.

Several simulations of the (0001) reflection were studied in the same Be crystal. The calculated loci for MBR in the neighborhood of $\theta \approx 11.0^\circ$ are shown in the upper part of Fig. 5. These curves have the same doubling and symmetry as those in Fig. 4. The intensity curve for $\alpha = 30^\circ$ shown in the lower part of Fig. 5 is not a directly observed curve; it is the result of subtracting the gadolinium-filtered intensity from that passing through a *thin* cadmium filter. The net effect is to remove the second, third, and fourth orders, all of which made appreciable contributions to the unfiltered beam. The Ge(111) reflection of the auxiliary crystal was used in the parallel position. Detailed measurements using several Gd, Cd, and Er filters were made at the simulation peaks and at the valley points A and B. It should be noted that these valleys in the (0001) intensity are wider than those for (0003). For comparison a similar set of filter measurements at the same wavelengths was again made on the

ordinary (0002) reflection. The intensity ratios determined by means of a least-squares analysis of the filter data are given in lines 4 and 5 of Table I, where the unresolved pair of peaks near $\theta = 11.7^\circ$ are lumped together.

V. MEASUREMENTS OF GERMANIUM REFLECTIONS

Detailed calculations have shown that approximately 80 simulated reflections in Ge are potentially suitable for high-resolution monochromatization.² This crystal is of considerable interest as a monochromator because it is available in large, almost perfect pieces.

The specimen used in the present measurements had the shape of an irregular slab with average dimensions $\approx 7 \text{ cm} \times 3 \text{ cm} \times 1 \text{ cm}$ (height, width, thickness). The angular width of one of its {111} reflections was $\Delta\theta \approx 0.02^\circ$; thus, it was rather far from a perfect crystal, although an order of magnitude better than the Be specimen. The [011] axis was vertical, and the plane of scattering horizontal. In Fig. 6 this orientation corresponds to $\alpha = 45^\circ$. The crystal was used in an asymmetrical transmission geometry (Laue case).

Measurements were made on simulations of the forbidden (200) reflection near $\theta = 14.5^\circ$ (see Fig. 6). Among the curves in the upper part of the figure, which show the loci of MBR, are two that are approximately vertical. These represent simulations of the (200) reflection which are potentially suitable for high-resolution monochromatization. The lower part of Fig. 6 shows the intensity observed in a special double-crystal traverse without any filters. Because of the greatly increased perfection of the crystal, it was necessary to use much smaller steps than for the Be specimen. Instead of traversing the entire neighborhood, measurements were concentrated in regions of particular interest; that is, the pair of narrow peaks, one wide peak, and the valley points A and B where only higher-order contamination was to be expected. In addition to two high-resolution peaks these unfiltered

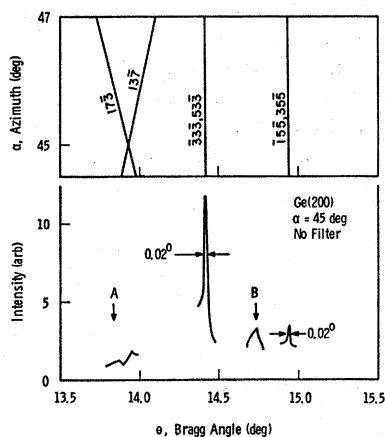


FIG. 6. Simulated Ge(200) reflections near $\theta = 14.5^\circ$. The double-crystal intensity curves in the lower part show two high-resolution simulations and the accompanying order contamination observed without filters.

data indicate a large and extremely variable background of higher-order neutrons. The apparent peaks near A and B represent structure in this background. Additional detailed measurements using Gd, Cd, Er, and Ir filters were made at the narrow peaks and at points A and B. Reference measurements of the "ordinary" (400) reflection were made with filters at the same wavelengths. All of these data were taken in the parallel position relative to the auxiliary crystal. After a least-squares analysis which had to remove three contaminating orders, the intensity ratios were formed; they are given in lines 6 and 7 of Table I.

To check the angle scale of the third arm of the spectrometer and the reproducibility of its angular settings, the precisely calculated quantity 4θ for the high-resolution peaks was measured by rotating the specimen crystal and arm from the antiparallel to the parallel positions. These measurements disclosed an unexpected "twisting" motion of the spectrometer, which was subsequently determined optically to be 0.014° . When corrected for this effect, the measured value of 4θ for the (533,333) simulation was $57.69 \pm 0.01^\circ$, compared to the calculated value of 57.68° .

VI. DISCUSSION

The results on intensities summarized in Table I require further comment. We note first that the ratios of simulated to ordinary intensities fall in the range of $1/60$ to $\frac{1}{5}$. The Ge(200) reflections appear to have the largest values, perhaps because of a smaller mosaic. It must be emphasized that the exact numerical values are not very important. In addition to the difficulties mentioned in Sec. II, it is known that the path lengths of the various beams in the crystal strongly affect the intensity of MBR beams.⁵ Thus caution must be used in applying these results to crystals having their size,

shape, or surface orientation greatly different from those of the present specimens.¹¹

The ratios involving intrinsic intensities must be considered separately for each of the forbidden reflections. For the Be(0003) reflection the filter analyses indicate an intrinsic intensity $\approx 1/400$ of the simulated intensities. However, consideration of Fig. 4 shows that the measurements of intrinsic intensities were made in rather narrow valleys. Thus, it is possible that some of the intensity attributed to intrinsic reflection is really due to the tails of simulation peaks. The filter analyses of the Be(0001) data indicate a net value of intrinsic intensity smaller than its statistical uncertainty (standard deviation). The tabulated ratios are based on this uncertainty and are shown as lower limits. We thus conclude that the simulated intensities of the forbidden reflections in this Be specimen are at least a few hundred times greater than the intrinsic intensities.

Analogous conclusions for the Ge reflections are not nearly so strong. Although the filter analyses of the Ge(200) intensity indicate no intrinsic component, the statistical uncertainties are relatively much larger than for Be because of much smaller counting rates and substantial order contamination. Thus we may conclude only that the simulated intensities in Ge are at least a few tens of times greater than the intrinsic intensities. More definitive measurements of this ratio will require more effective methods for handling the problem of order contamination.

ACKNOWLEDGMENT

Thanks are due to B. H. Duane for providing the computer program used in the least-squares analysis.

¹¹ However, it should be remarked that the intensity ratios for small crystals reported in Ref. 5 fall in approximately the same range as those reported here.